Deep-subwavelength nanohole arrays embedded in nanoripples fabricated by femtosecond laser irradiation

Vanthanh Khuat,[1,2] Jinhai Si,[1,*] Tao Chen,[1] and Xun Hou[1]

[1]*Key Laboratory for Physical Electronics and Devices of the Ministry of Education & Shaanxi Key Laboratory of Information Photonic Technique, School of Electronics & Information Engineering, Xi'an Jiaotong University, No. 28, Xianning West Road, Xi'an 710049, China*

[2]*Le Quy Don Technical University, No. 100, Hoang Quoc Viet Street, Hanoi 7EN-248, Vietnam*

**Corresponding author: jinhaisi@mail.xjtu.edu.cn*

Received November 13, 2014; revised December 10, 2014; accepted December 11, 2014; posted December 11, 2014 (Doc. ID 226844); published January 9, 2015

We report on the formation of deep-subwavelength nanohole arrays embedded in silicon carbide nanoripples fabricated by an 800 nm femtosecond laser in an underwater environment. The period of the nanoripples is about 500 nm. The ripples are perpendicular to the polarization direction of the incident laser. The diameter of the holes is about 30 nm, and the period of the hole array is about 60 nm. Nanoripple formation is attributed to interference of the incident laser and a laser-induced plasma wave. Nanohole array formation is attributed to the formation of channel plasmon polaritons in the laser-induced nanogrooves associated with the nanoripples.

OCIS codes: (140.3390) Laser materials processing; (160.6000) Semiconductor materials; (220.4241) Nanostructure fabrication; (140.7090) Ultrafast lasers.

http://dx.doi.org/10.1364/OL.40.000209

The laser has become an important tool for micro- and nanomachining. Specifically, the femtosecond laser has proved to be a versatile micromachining tool because it can deposit energy into a transparent material through high-order nonlinear absorption [1–3]. It has been applied to drilling, patterning, and synthesizing various types of micro- and nanostructures in both metals and semiconductors [4–10]. Among these structures, laser-induced nanoripples have gained considerable attention from researchers owing to their potential applications in photovoltaics, surface texturing, and 3D data storage. Accordingly, there have been many studies on the fabrication of nanoripples both on surfaces and in bulk [11–14].

The formation of nanoripples on a surface would change how incident laser light interacts with the material, and the physical picture would be more complicated [15]. In particular, since the width of the laser-induced nanogrooves is about 10–50 nm [16], which is much smaller than the incident laser wavelength, light waves cannot propagate in such a small structure because of the diffraction limit. Therefore, it can be expected that surface plasmon polaritons (SPPs) could be generated and confined in the nanogrooves, which would induce much smaller nanostructures on the surface of materials. However, most recent works focused only on characterizing the morphology and formation mechanism of the nanoripples. Few studies have been reported on the nanostructures induced by the SPPs in the laser-induced nanogrooves.

In this Letter, we report on the observation of deep-subwavelength nanohole arrays embedded in the nanogrooves of nanoripples on a silicon carbide (SiC) surface irradiated with an 800 nm femtosecond laser in an underwater environment. The phenomenon is attributed to the formation of channel plasmon polaritons (CPPs) in the nanogrooves. Clear nanoripples were formed first; then the deep-subwavelength nanohole arrays appeared with decreasing laser scanning velocity. A scanning electron microscope (SEM) equipped with an energy-dispersive x-ray spectroscope (EDS) was employed to characterize the morphology and chemical composition of the nanoripples and nanohole arrays. We proposed a possible mechanism to explain the formation of the nanohole arrays. Additionally, we discussed the influence of the incident laser polarization direction on the nanohole arrays.

The experimental setup (Fig. 1) consists of a femtosecond laser source, an attenuator, a neutral density filter, a mechanical shutter, an *xyz* movable stage, a computer, and a CCD camera. The laser used was an amplified Ti:sapphire femtosecond laser system (Coherent Inc.,

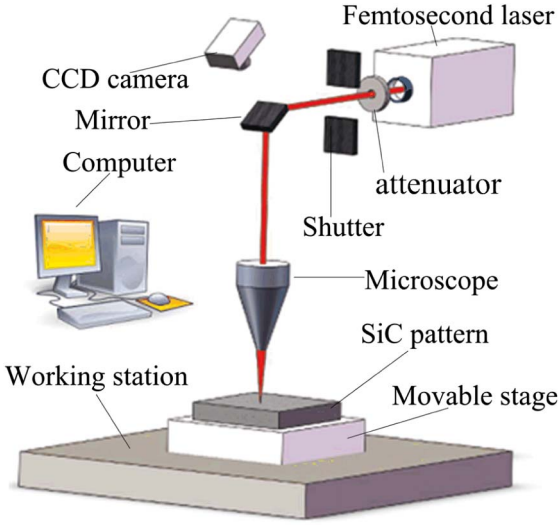

Fig. 1. Experimental setup for using laser irradiation to fabricate patterns on SiC.

USA) with a pulse duration of 150 fs, wavelength of 800 nm, and repetition rate of 1 kHz. The attenuator provided a convenient way to adjust the laser energy, and the mechanical shutter was employed to control the access of the laser beam. The movable stage, on which the SiC sample could be mounted, was controlled by a computer program and allowed us to fabricate structures on the patterns with high precision. The CCD camera was connected to a computer for clear online observation of the SiC pattern surface during fabrication. A 10× microscope objective with numerical aperture (NA) of 0.3 was employed to focus the laser onto the surface of the pattern. The diameter of the spot on the pattern was about 10 μm.

In our experiments, a 6H-SiC pattern 350 μm in thickness was used. First, it was cleaned in acetone and deionized water with an ultrasonic field for 10 min each; then it was immersed in a smaller water pool before being mounted on the movable stage. The laser beam was focused onto the pattern via an optical microscope objective lens. During fabrication, the surface of the SiC pattern could be seen either via optical microscope or on the computer screen connected to the CCD camera. After laser irradiation, an SEM equipped with an EDS was employed to study the morphology of the structures on the SiC surface.

Figure 2 shows the nanoripples and deep-subwavelength nanohole arrays formed on the SiC surface. The average laser power was 15 mW. At a laser scanning velocity of 2000 μm/s, corresponding to about 80% overlap between two successive laser pulses, clear nanoripples were formed on the surface of the pattern, as shown in Fig. 2(a). The period of the nanoripples is about 500 nm, and the width of the nanogrooves is about 15 nm. The nanoripples were perpendicular to the laser polarization direction. As the laser scanning velocity was decreased to 1500 μm/s, corresponding to about

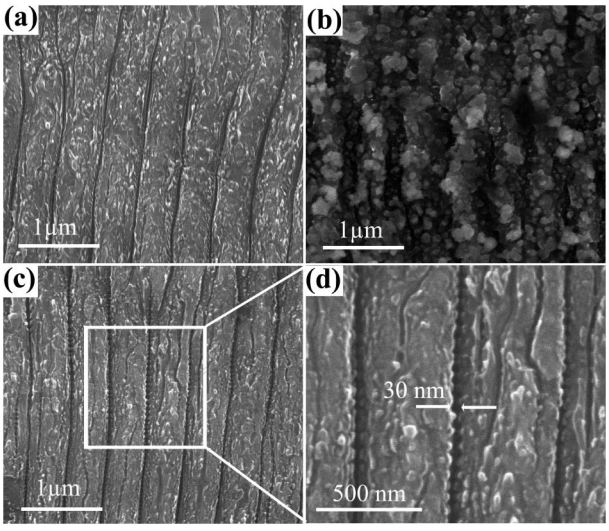

Fig. 2. SEM images of the morphology of nanostructures on the surface of SiC after irradiation with an 800-nm femtosecond laser: (a) in an under-water environment, (b) in ambient air, (c) deep-subwavelength nanohole arrays embedded in the nanogrooves, and (d) magnified view of the nanohole arrays.

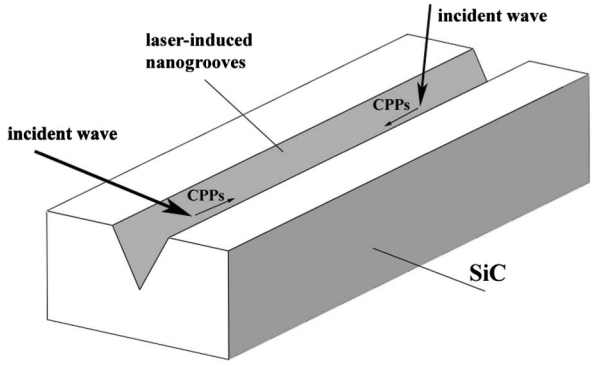

Fig. 3. Formation mechanism of the nanohole arrays in a nanogroove.

90% overlap between two successive laser pulses, deep-subwavelength quasi-periodic nanohole arrays with a period of 60 nm and diameter of 30 nm were formed in the nanogrooves, as shown in Fig. 2(c). Note that the nanoholes are much smaller than the wavelength of the incident laser, which is 800 nm. Such deep-subwavelength nanohole arrays have not been reported elsewhere. We attributed their formation to the guiding effect of the CPPs on the nanogrooves associated with the nanoripples [17,18]. Figure 3 illustrates the formation mechanism of the nanohole arrays in a nanogroove. For convenience, the laser-induced nanogroove is assumed to be a V-shape groove. When being irradiated by femtosecond laser, the nanogrooves were formed first; the nanogrooves effectively coupled incident light and converted it into a plasma wave [19]. At this stage, the SiC surface should behave like a metal [15]. Further, the nanogrooves supported the propagation of CPPs. The deep-subwavelength nanohole arrays can be attributed to the periodic distribution of the intensity of the CPPs along their propagation direction. The periodic distribution of the CPPs is probably due to the interference of two CPPs propagating in opposite directions inside the nanogrooves. It is worth mentioning that the incident laser beam is symmetric, and the laser beam spot focused by the microscope is much larger than the nanoripples. Therefore, CPPs could probably be generated and propagate in opposite directions, interfering with each other to form the periodic distribution of CPPs along the nanogrooves.

We attribute the formation of the nanoripples to interference between the incident laser beam and the laser-induced surface plasma wave [15]. The period of the nanoripples can be calculated as follows: $\Lambda = \lambda/(\lambda/\lambda_{sp} \pm \sin\theta)$, with $\lambda_{sp} = \lambda(\frac{\xi' + \xi_d}{\xi' * \xi_d})^{1/2}$, where Λ is the period of the nanoripples; λ is the incident laser wavelength; θ is the incident angle; λ_{sp} is the wavelength of the laser-induced plasma wave; ξ' is the real part of the dielectric constant of the laser-induced plasma, which may fulfill the condition for a metal, $\xi' < -1$; and ξ_d is the dielectric constant of dielectric material ($\xi_d = 1.3$ for water). According to the formula above, the period of the nanoripples reaches its maximum λ_{sp} at normal incidence. Note that the period of the ripples is slightly smaller than the result reported by the author of [20], in which the ripple period is about 600 nm. This is

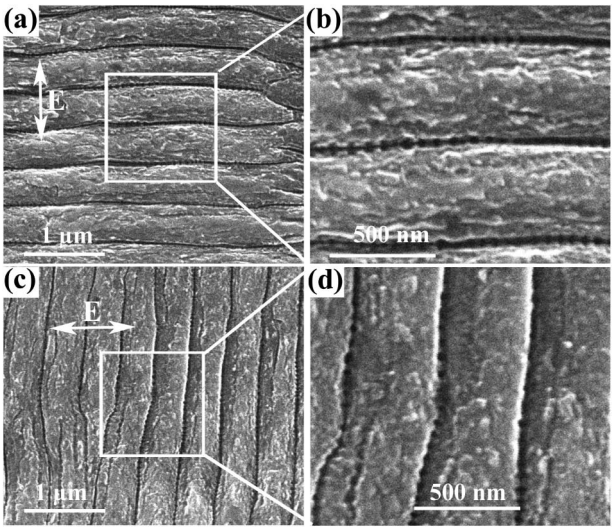

Fig. 4. SEM images of morphology of SiC deep-subwavelength nanohole arrays embedded in nanogrooves fabricated in an underwater environment as the laser polarization direction changes: (a) **E** perpendicular to the scanning direction, (b) magnified view of the deep-subwavelength nanoholes in (a), (c) **E** parallel to the scanning direction, and (d) magnified view of the deep-subwavelength nanoholes in (c).

because the ξ_d value of water is 1.3, whereas that of air is 1; consequently, according to the formula above, the λ_{sp} induced in water is smaller than that induced in air. It is worth mentioning that such clear nanoripples and nanogrooves are difficult to achieve when fabricating SiC in ambient air, because under irradiation in ambient air, the debris redeposited on the surface during laser treatment could scatter the incident light, severely damaging the structure of the nanopatterns on the surface. Figure 2(b) shows a typical surface irradiated with the same laser parameters in ambient air. In contrast, underwater micromachining has several advantages, such as higher plasma pressure due to confinement, more effective cooling of the workpiece and ejected material, and a smaller focal spot size [21]. Therefore, as the pattern was immersed in water, clear nanoripples and nanogrooves were easily fabricated.

We also studied the influence of the laser polarization direction (**E**) on the deep-subwavelength nanohole arrays. Figure 4 shows the morphology of the nanohole arrays and ripples with **E** perpendicular and parallel to the laser scanning direction. Nanohole arrays were formed in both cases, and their direction changed with the polarization direction of the incident laser. This is because the direction of the nanogrooves changes with the polarization direction, and as discussed above, the formation of the nanohole arrays is due to the formation of nanogrooves, which further emphasize the guiding effect of the CPPs. Therefore, the direction of the nanohole arrays changes with the polarization direction of the incident laser. This also supports the idea that the formation of nanogrooves is very important to the formation of nanohole arrays; this is why the phenomenon could not be seen when patterns on SiC were fabricated in air.

Since the wavelength of the fundamental mode of CPPs increases with the increase of incident laser wavelength [22], it is expected that the period of the nanohole array increases with the increase of the laser source wavelength, and the diameter of the holes may also change due to the redistribution of energy in the nanogrooves. However, as the wavelength of the laser source changes, the absorption of the material would be changed, leading to the change in geometric properties of the laser-induced nanogrooves, which also have great influence on the CPPs. Thus, much effort is needed in future work to understand the influence of the laser source wavelength on the nanohole arrays and verify the proposed model in the present work.

In conclusion, we observed the formation of deep-subwavelength nanohole arrays embedded in nanogrooves associated with nanoripples fabricated under irradiation by an 800 nm femtosecond laser in an underwater environment. Clear nanoripples were formed first; then, as the laser scanning velocity decreased, nanohole arrays appeared in the nanogrooves. The period of the nanoripples is about 500 nm. The ripples are perpendicular to the polarization direction of the incident laser. The size of the holes is about 30 nm, and the period is about 60 nm. Nanoripple formation can be attributed to interference of the incident laser and the laser-induced surface plasma wave. Further, the formation of the deep-subwavelength nanohole arrays is attributed to the guiding effect of CPPs on the nanogrooves associated with the nanoripples.

The authors gratefully acknowledge the financial support for this work provided by the National Natural Science Foundation of China (NSFC) under Grant No. 61235003, and the National Basic Research Program of China (973 Program) under Grant No. 2012CB921804. This work also was supported by the Collaborative Innovation Center of Suzhou Nano Science and Technology. The authors also sincerely thank Ms. Dai at International Center for Dielectric Research (ICDR) in Xi'an Jiaotong University for the support of SEM and EDS measurements.

References

1. R. R. Gattass and E. Mazur, Nat. Photonics **2**, 219 (2008).
2. C. B. Schaffer, A. Brodeur, and E. Mazur, Meas. Sci. Technol. **12**, 1784 (2001).
3. C. B. Schaffer, A. Brodeur, J. F. García, and E. Mazur, Opt. Lett. **26**, 93 (2001).
4. A. Weck, T. H. R. Crawford, D. S. Wilkinson, H. K. Haugen, and J. S. Preston, Appl. Phys. A **90**, 537 (2008).
5. A. Y. Vorobyev, V. S. Makin, and C. J. Guo, Appl. Phys. **101**, 034903 (2007).
6. V. Khuat, Y. Ma, J. Si, T. Chen, F. Chen, and X. Hou, Appl. Surf. Sci. **289**, 529 (2014).
7. B. Pecholt, G. Saurabh, and M. Pal, J. Laser Appl. **23**, 012008 (2011).
8. M. Farsari, G. Filippidis, S. Zoppel, G. A. Reider, and C. Fotakis, J. Micromech. Microeng. **15**, 1786 (2005).
9. S. Zoppel, M. Farsari, R. Merz, J. Zehetner, G. Stangl, G. A. Reider, and C. Fotakis, Microelectron. Eng. **83**, 1400 (2006).
10. Y. Dong, C. Zorman, and P. Molian, J. Micromech. Microeng. **13**, 680 (2003).
11. V. Khuat, T. Chen, B. Gao, J. Si, Y. Ma, and X. Hou, Appl. Phys. Lett. **104**, 241907 (2014).

12. X. D. Guo, R. X. Li, Y. Hang, Z. Z. Xu, B. K. Yu, Y. Dai, and X. W. Sun, Appl. Phys. A **94**, 423 (2009).
13. V. R. Bhardwaj, E. Simova, P. P. Rajeev, C. Hnatovsky, R. S. Taylor, D. M. Rayner, and P. B. Corkum, Phys. Rev. Lett. **96**, 057404 (2006).
14. Y. Shimotsuma, P. G. Kazansky, J. Qiu, and K. Hirao, Phys. Rev. Lett. **91**, 247405 (2003).
15. M. Huang, F. Zhao, Y. Cheng, N. Xu, and Z. Xu, ACS Nano **3**, 4062 (2009).
16. R. Buividas, L. Rosa, R. Šliupas, T. Kudrius, G. Šlekys, V. Datsyuk, and S. Juodkazis, Nanotechnology **22**, 055304 (2011).
17. S. I. Bozhevolnyi, V. S. Volkov, E. Devaux, and T. W. Ebbesen, Phys. Rev. Lett. **95**, 046802 (2005).
18. S. I. Bozhevolnyi, V. S. Volkov, E. Devaux, J. Y. Laluet, and T. W. Ebbesen, Nature **440**, 508 (2006).
19. C. Ropers, C. C. Neacsu, T. Elsaesser, M. Albrecht, M. B. Raschke, and C. Lienau, Nano Lett. **7**, 2784 (2007).
20. L. Gemini, M. Hashida, M. Shimizu, Y. Miyasaka, S. Inoue, S. Tokita, J. Limpouch, T. Mocek, and S. Sakabe, J. Appl. Phys. **114**, 194903 (2013).
21. A. Kruusing, Opt. Laser. Eng. **41**, 307 (2004).
22. D. F. P. Pile and D. K. Gramotnev, Opt. Lett. **29**, 1069 (2004).